海洋安全學會誌 第 4 卷 第 2 號, pp. 1~12, 1998. 7.

論 文

A Study on the Simulation of Grounding of Double Hull Tanker using LS/DYNA3D

*Sang-Gab Lee**

LS/DYNA3D를 이용한 이중선체 유조선의 좌초에 관한 연구

이 상 갑*

〈Contents〉

Abstract

This paper describes a series of numerical simulations of grounding accidents of four 40,000 DWT Conventional and Advanced Double Hull tanker bottom structures using LS/DYNA3D. The overall objective of this study is to understand the structural failure and energy absorbing mechanisms during grounding events for candidate double hull tanker bottom structures, which lead to the initiation of inner shell rupture and cause the kinetic energy dissipation to bring the ship to a stop. These numerical simulations of the grounding events will contribute to future improvements in tanker safety at the design stage.

요 약

이 논문에서는 LS/DYNA3D를 이용하여 40,000 DWT급의 재래식과 개량식 이중선체 유조선의 선저구

* 정회원, 한국해양대학교 조선해양공학부 부교수

조 4모델에 대한 좌초에 관한 일련의 수치 시뮬레이션에 대하여 기술하고 있다. 이 연구의 목적은 이중선체 유조선의 선저구조에 좌초가 발생하는 동안 이중선체의 내판이 찢어지기 시작하고 운동에너지가 소산되면서 선체가 정지되는 등의 구조적인 파손 및 흡수에너지의 역학적인 거동을 이해하는 것이다. 유조선의 좌초에 관한 본 연구의 수치 시뮬레이션을 통하여 설계단계에서의 안전도 개선에 이바지할 수 있을 것이다.

1. Introduction

Since the grounding of Exxon Valdez in 1989 focused the international attention on the oil spills, the United States of America required a double hull for future tankers in 1990 and IMO adopted similar, though a little bit relaxed regulations in 1992. Whereas intensive researches on collision have been performed[1~4], very little has been known about structural damage on the grounding events[5]. Further research on grounding is necessary to come up with design regulations and recommendations for tanker design to reduce the risk of oil spilling.

Several large scale oil tanker grounding experiments performed by the Carderock Division of Naval Surface Warfare Center (CDNSWC) as part of the Advanced Double Hull Technology Project[6~8]. Several design models were evaluated for the 30,000~40,000 ton tanker range at approximately one-fifth scale, using the Grounding Test Machine with a test vehicle(or sled) and impact area. Sled built on twin railcars carried the grounding model down an inclined set of railroad tracks to an impact area at a sled velocity of 6.17~7.20 m/sec (12~14 knots). A steel grounding rock included in the impact area was a 90 degree cone with a radius spherical tip. The installation and orientation of the inclined grounding model is shown in Fig. 1 with 7.4 degrees of attack angle and the entry/exit height of the rock tip.

There are generally two parameters of concerns for a systematic comparison of the

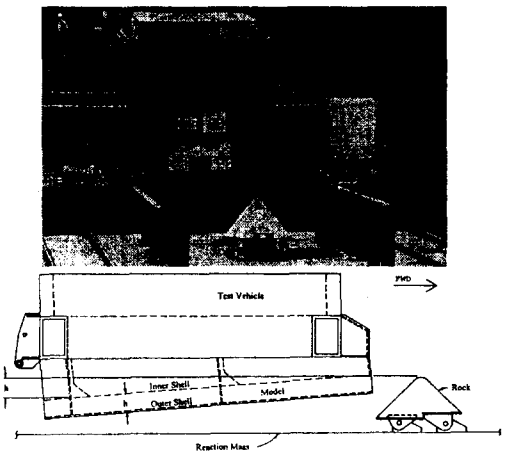

Fig. 1 Installation of grounding model[6~8]

grounding resistance of various double hull bottom designs: The first one is the amount of vertical intrusion(the height of rock tip above the keel) without inner shell rupture, and the second, the amount of energy dissipation which is characteristic of a given structure with inner shell rupture[7]. It is desirable to estimate the crashworthiness of double hull bottom structures against grounding comparing their occurrence times, distances from front bulkhead, heights of rock tip and energy absorption capacities at the initial inner shell ruptures with each other.

In this study, four 40,000 DWT Conventional and Advanced Double Hull tanker bottom structures are used as the numerical simulation models of grounding accidents using LS/DYNA3D with the same arrangements, which are scaled the experimental models conducted by CDNSWC by the scale factor 5.33 for the full scale structure: PAUL BUCK,

CONV/PD328, ADH/PB, and ADH/PD328 models[6~8]. The numerical simulation models are changed a little bit from the experimental ones with the same sizes and impact speed 7.20 m/sec(14.0 knots) for systematic comparisons with each other.

The overall objective of this study is to understand the structural failure and the energy absorbing mechanisms during grounding events for candidate double hull tanker bottom structures, which lead to the initiation of inner shell rupture and cause the kinetic energy dissipation to bring the ship to a stop. This numerical simulations of inner shell rupture due to a grounding accidents will contribute to future improvements in tanker safety at the design stage.

2. Simulation Models and Validation of LS/DYNA3D

2.1 Simulation models

Figure 2 shows four numerical simulation models: two Conventional double hull tanker bottom designs, and two Advanced (unidirectional) Double Hull(ADH) tanker bottom systems. The first Paul Buck model, as shown in Fig. 2(a), was the first experiment represented by a Conventional T-5 Double Hull tanker bottom with transverse and longitudinal framing[6]. The second CONV/PD328 model, as illustrated in Fig. 2(b), represented the Conventional Double Hull design, whose bottom structure is identical to the MARAD PD328[7,8]. The third Advanced Double Hull model ADH/PB, in Fig. 2(c), was an early conceptual design for comparison to the conventional frame, T-5 Paul Buck class. This is characterized by relatively wide spacing of longitudinal webs, conventional plate/stiffener bulkheads, and thinner plating for the inner shell[7,8]. As shown in Fig. 2(d), the fourth ADH/PD328 model was a rigorously designed alternative to the conventional MARAD PD328,

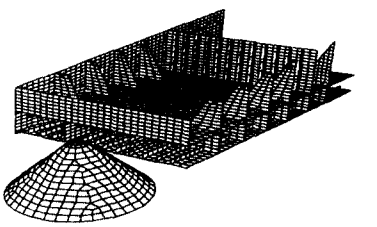

(a) PAUL BUCK (Element No. 10,000)

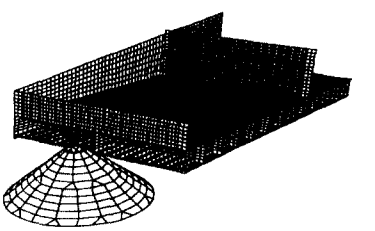

(b) CONV/PD328 (Element No. 22,000)

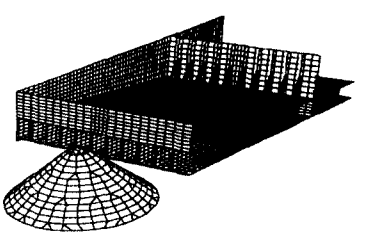

(c) ADH/PB (Element No. 20,000)

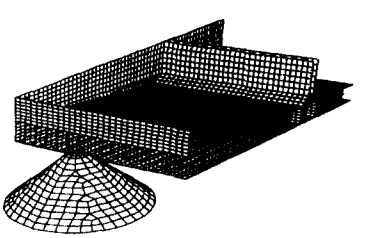

(d) ADH/PD328 (Element No. 16,000)

Fig. 2 Finite element mesh of grounding models

which is characterized by a tighter spacing of longitudinal webs, double-plate transverse bulkheads with haunted stools[7,8].

Figure 2 shows plots of finite element meshes of the above mentioned simulation models and grounding rock, which consist of the double bottom structure beneath one and half oil tanks, the forward and aft transverse bulkheads, and heavy sideplates. All members of grounding models and grounding rock are meshed using around 10,000~22,000 shell elements. The mass of the sled is controlled by rigid plate on the top of the double hull model, which is invisible together with left sideplate as shown in Fig. 2. The grounding rock is modeled to be rigid and the double hull model is restrained to move straightly forward, and not upward/downward. Their general dimensions are also illustrated in Table 1, which are scaled by the scale factor 5.33 for the full scale structure.

Table 1 Dimensions of grounding models

Item (m)	PAUL BUCK	CONV/PD328	ADH/PB	ADH/PD328
Width	13.538	13.538	13.325	13.538
Length	19.507	19.507	19.507	19.507
Fwd height	4.482	4.642	4.673	4.212
Bottom height	1.972	1.972	1.972	1.972
Shell thck.	0.016	0.016	0.016	0.016
Stiffener thck.	0.016~0.017	0.016	0.016	0.016
Trans. web thck.	0.016	0.016	—	—
Longi. web thck.	0.016	0.0123	0.016	0.016
Side plate thck.	1.35	1.35	1.35	1.35

Strain rate dependent isotropic plasticity material type is employed for the double hull bottom structures. This material type is suitable for the consideration of the material dynamic effect. Every finite element is due to be eliminated for rupture process of structures when plastic strain reaches to the failure value, 0.25 in this study. The material properties used in this study are shown in Table 2.

Table 2 Material properties of grounding models

Density	7850.0 Kg/m3
Modulus of elasticity	210 GPa
Poisson's ratio	0.28
Yield stress (mild steel)	250 MPa
Ultimate stress (mild steel)	400 MPa
Dynamic yield stress constants[9]	40.4, 5.0
Failure plastic strain	0.25

2.2 Validation of LS/DYNA3D

Figure 3 shows the comparison of numerical simulation result with CDNSWC experimental one (PAUL BUCK, one-fifth scale) about the horizontal impact force (plate resisting force) vs. the sled position. Compared to the experimental result, it can be said that the numerical simulation result is satisfactory and that LS/DYNA3D is sufficient to perform the following grounding problems.

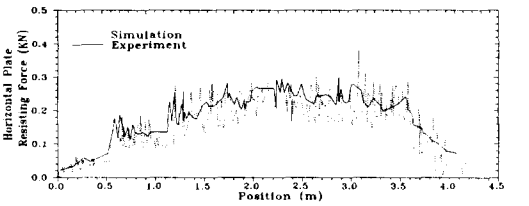

Fig. 3 Comparison of numerical simulation and experimental results[6]

3. Numerical Simulations

Figures 4~7 show the rupture configurations of the grounding models by the grounding rock,

Table 3 Informations at initiation of inner shell rupture of grounding models

Item (m)	PAUL BUCK	CONV/PD328	ADH/PB	ADH/PD328
Time(sec)	2.02	2.48	2.00	2.20
Rock tip position(m)	13.962	17.001	13.935	14.911
Rock tip height(m)	3.190(1.618)	3.565(1.805)	3.166(1.605)	3.329(1.703)
Vertical Collision Force(MN)	35.4363	51.4841	30.627	47.8084
Fore/Aft Collision Force(MN)	23.347	44.008	20.985	35.763
Absorbed Energy(MN-m)	240.631	249.432	176.168	330.987
Rock tip position(m), t=4.5sec	27.700	28.051	28.436	26.062
Velocity(m/sec), t=4.5sec	4.933	4.890	5.244	3.950

such as (a) inner shell rupture initiation, (b) bottom structure rupture at the initiation of inner shell rupture, (c) webs and frames rupture at the initiation of inner shell rupture, and (d) inner shell rupture initiation at final simulation time(4.5 sec). Figures 8 and 9 show the plots of vertical and fore/aft collision forces with respect to the rock tip position for the grounding models until final simulation time t=4.5sec, respectively. Total absorbed energy and velocity histories with an initial velocity 7.20 m/sec(14 knots) are also plotted with respect to the rock tip position in Fig. 10. Figure 11 shows each member absorbed energy of the grounding models with respect to the rock tip position. Dot point(·) on the graphs through Figs. 8~11 indicates the state of initiation of inner shell rupture. Many informations at the initiation of inner shell rupture of grounding models are summarized in Table 3, such as occurrence time, distances from front bulkhead, height of rock tip, vertical and fore/aft collision forces, absorbed energy, addition to the rock tip position and velocity at final simulation time.

3.1 PAUL BUCK model

The vertical and fore/aft collision forces of PAUL BUCK model plotted in Figs. 8(a) and 9(a) show that as rock tip passes 4 transverse webs and aft bulkhead, very distinctive force fluctuations clearly mark the locations of these webs and aft bulkhead at approximately 5.722(0.80), 8.216(1.16), 11.326(1.62), 14.580(2.12) and 21.310m(3.25sec) from the rock tip position zero reference. The initial crack in the inner shell begins at 13.962m(2.02sec) distance with 3.190m of rock tip height after rock tip ruptures the 3rd transverse web, as shown in Figs. 4(a)~(c). This phenomena can be expressed that the crack in the inner shell results from high membrane stressing in the inner shell rather than the transmission of a vertical crack propagation from transverse web to inner shell.

The total absorbed energy and velocity histories can be seen in Figs. 10(a) and (b), respectively. The following members are contributed to the crashworthiness, such as mainly outer shell and transverse webs, and partly longitudinal webs, inner shell, outer and inner shell stiffeners, and longitudinal web stiffeners, as shown in Fig. 11(a).

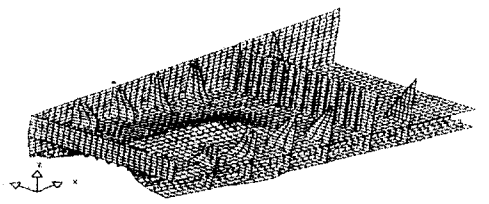

(a) inner shell rupture initiation(t=2.02sec)

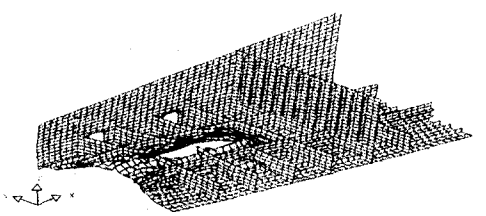

(b) bottom structure rupture(t=2.02sec)

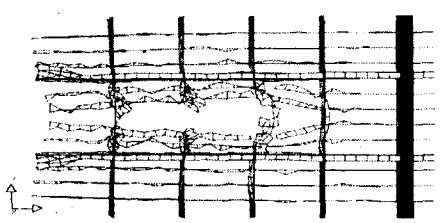

(c) webs/frame rupture(t=2.02sec)

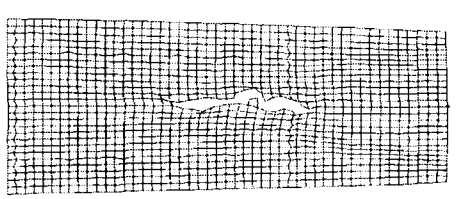

(d) inner shell rupture at final time(t=4.5sec)

Fig. 4 Rupture configuration of grounding model, PAUL BUCK

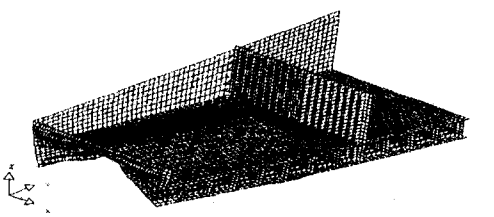

(a) inner shell rupture initiation(t=2.48sec)

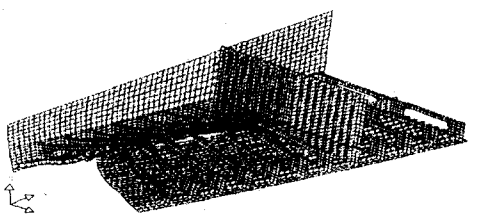

(b) bottom structure rupture(t=2.48sec)

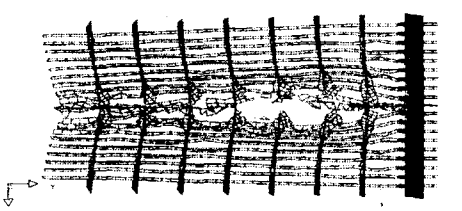

(c) webs/frame rupture(t=2.48sec)

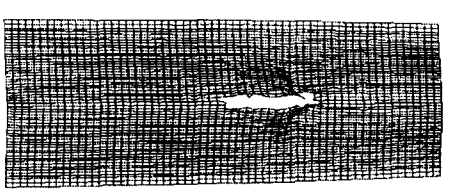

(d) inner shell rupture at final time(t=4.5sec)

Fig. 5 Rupture configuration of grounding model, CONV/PD328

3.2 CONV/PD328 model

In contrast to the case of PAUL BUCK model, the vertical and fore/aft collision forces of CONV/PD328 model in Figs. 8(b) and 9(b) show that distinctive force fluctuations does not clearly mark the locations of 7 transverse webs. Collision forces increase sharply after the 7th transverse web rupture at 16.498m(2.40sec) and then inner shell rupture at 17.001m(2.48sec), as shown in Figs. 5(a)~(c). The vertical collision force of the latter are partly larger only at the initiation of inner shell rupture and aft bulkhead rupture than that of the former. As shown in Fig. 10(a), the total absorbed energy of the

former is generally larger than that of the latter, but their discrepancies decrease as the simulation time is going to the end. It also can be seen from Fig. 10 that tendencies of total energy and velocity are inverse with each other.

As shown in Fig. 11(b), almost the same members of CONV/PD328 model as the PAUL BUCK model are contributed to the crashworthiness except the sequence of inner shell and outer shell stiffeners, and differences of their contributions are not much rather than those of PAUL BUCK. Even though total absorbed energy of the former is generally less than that of the latter, the initiation of inner shell rupture of the latter occurs at further longer distance of rock tip position and time compared to that of the former with much higher collision forces. As shown in Figs. 4(c), 5(c), 6(c) and 7(c), the side bottom stiffeners and transverse webs of the latter can be seen to bend largely, which means that this bottom structure is better connected against crash than any other models. This might be guessed that the bottom structure system of the CONV/PD328 model is more flexible and better crashworthy at the initiation of the inner shell rupture.

3.3 ADH/PB model

The tendency of vertical and fore/aft collision forces of ADH/PB model in Figs. 8(c) and 9(c) is almost similar to those of CONV/PD328, except small increase of vertical collision force of the former before and after the inner shell rupture and its large decrease after aft bulkhead rupture. From Figs. 10(a) and (b), total absorbed energy of the former is almost the same as that of the latter except partially less after aft bulkhead rupture, and is much

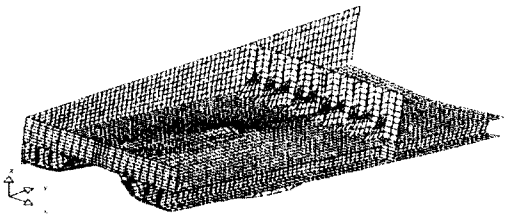

(a) inner shell rupture initiation(t=1.98sec)

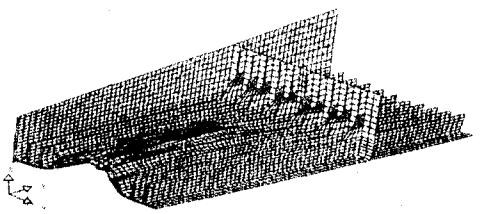

(b) bottom structure rupture(t=1.98sec)

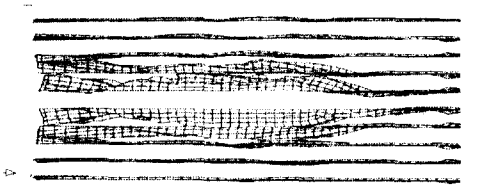

(c) webs/frame rupture(t=1.98sec)

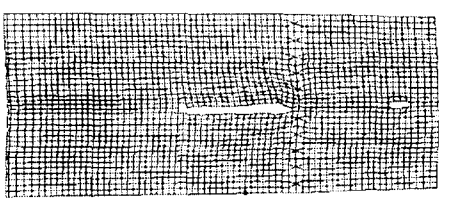

(d) inner shell rupture at final time(t=4.5sec)

Fig. 6 Rupture configuration of grounding model, ADH/PB

less than that of PAUL BUCK model. Rate of its velocity decrease is the lowest among all the models.

Figures 6(a)~(c) show that the initiation of inner shell rupture of ADH/PB model occurs at 13.935m(2.00sec) with 3.166m rock tip height, which is similar to the case of PAUL BUCK

model, 13.962m(2.02sec) and 3.190m. It can be seen that only the impacted longitudinal webs against the rock buckle without crash, which indicates that the bottom structures are not well connected against the crash. As shown in Fig. 11(c), the members of longitudinal webs and their stiffeners are more contributed to the crashworthiness than outer shell, differently to the previous convention models.

3.4 ADH/PD328 model

The vertical and fore/aft collision forces of ADH/PD328 model in Figs. 8(d) and 9(d) are generally the largest among all the models. As shown in Figs. 10(a) and (b), their total absorbed energies have the same trends as their collision forces, and rate of velocity decrease of the former is the steepest among all the models. This means this model is the best crashworthy against grounding events globally.

As shown in Figs. 7(a)~(c), however, the initiation of inner shell rupture of this model occurs at the shorter distance 14.911m(2.20sec) with the lower height of rock tip 3.329m than those of CONV/PD328, and therefore this bottom structure has a little bit poorer crashworthiness locally than the latter in spite of the globally superior crashworthiness. Similar bucked longitudinal webs to those of ADH/PB can be seen in Figs. 7(b) and (c), however much more longitudinal webs contribute to the resistance of buckling and rupture which might be caused by the narrower their arrangements than those of ADH/PB model. As shown in Fig. 11(d), the members of longitudinal webs and their stiffeners are more contributed to the crashworthiness than outer shell, similar to ADH/PB model.

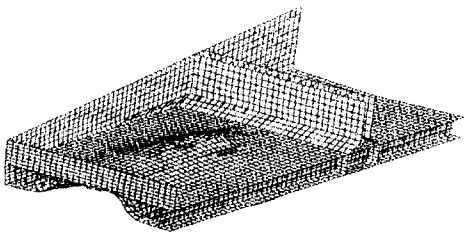

(a) inner shell rupture initiation(t=2.20sec)

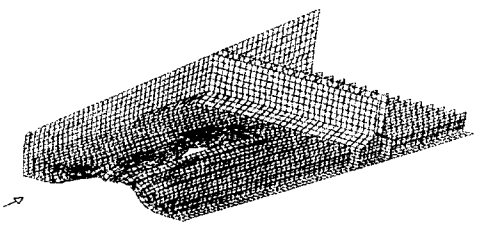

(b) bottom structure rupture(t=2.20sec)

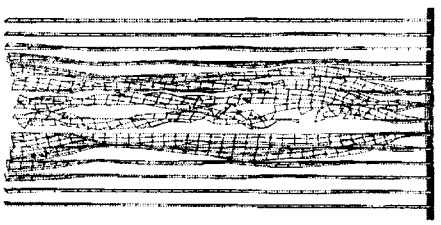

(c) webs/frame rupture(t=2.20sec)

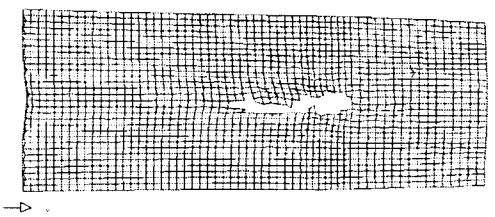

(d) inner shell rupture at final time(t=4.5sec)

Fig. 7 Rupture configuration of grounding model, ADH/PD328

From each inner shell rupture configuration at final simulation time(4.5 sec) of Figs. 4(d)~7(d), the inner shell rupture continues to the second

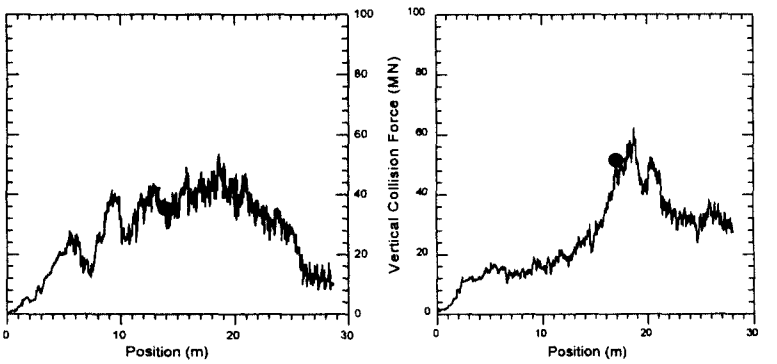

(a) PAUL BUCK (b) CONV/PD328

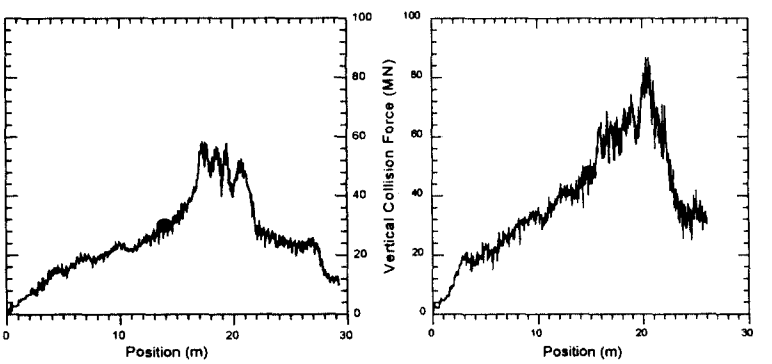

(c) ADH/PB (d) ADH/PD328

Fig. 8 Vertical collision force of grounding models

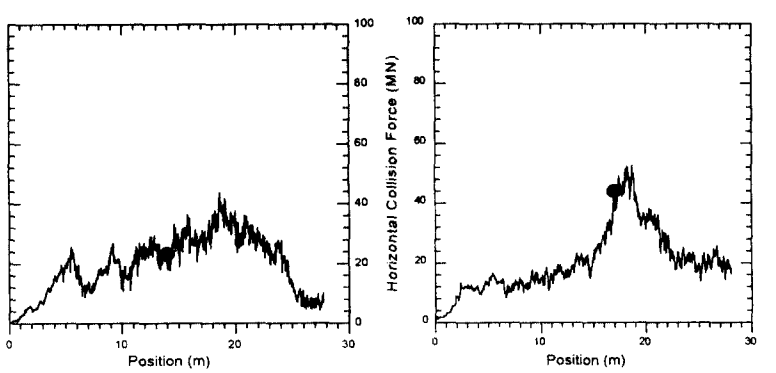

(a) PAUL BUCK (b) CONV/PD328

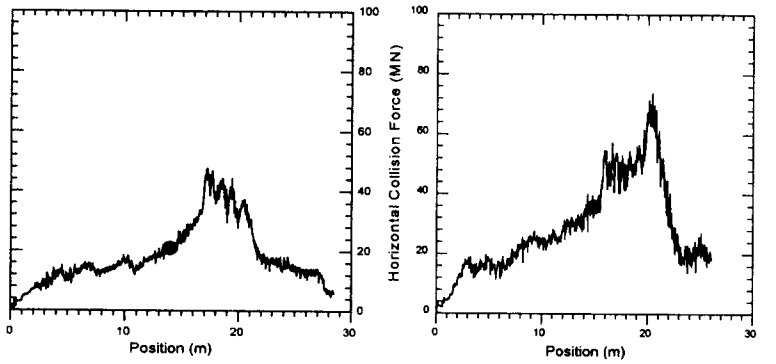

(c) ADH/PB (d) ADH/PD328

Fig. 9 Fore/Aft collision force of grounding models

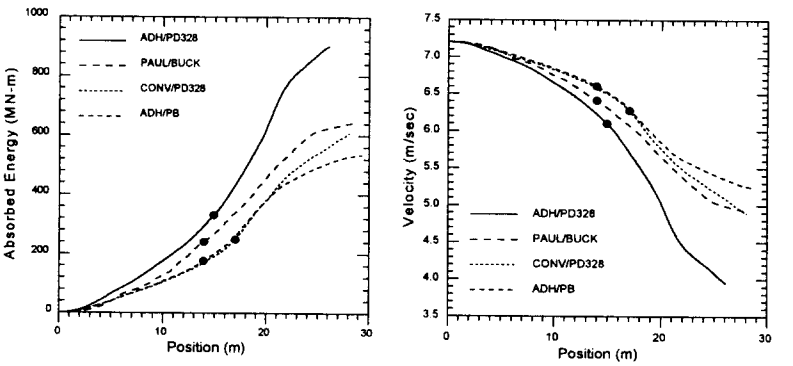

(a) Absorbed energy (b) Velocity

Fig. 10 Absorbed energy and velocity of grounding models

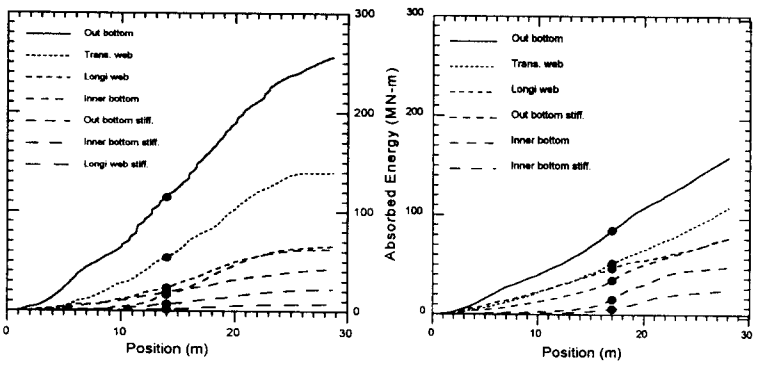

(a) PAUL BUCK (b) CONV/PD328

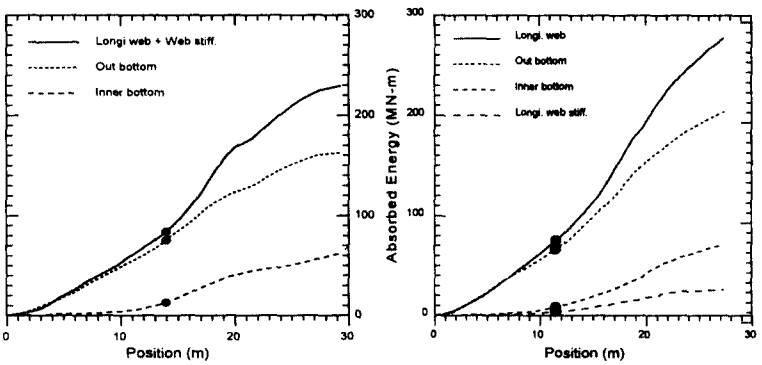

(c) ADH/PB (d) ADH/PD328

Fig. 11 Member absorbed energy of grounding models

tank partially except ADH/PD328, which might be the structural feature of its double-plate bulkhead to the bottom shell with haunted stool. This kind of bulkhead might contribute to the crashworthiness more with a tighter spacing arrangement of longitudinal webs globally.

4. Summary and Conclusion

A series of numerical simulations of grounding events of four 40,000 DWT Conventional and Advanced Double Hull tanker bottom structures have been performed using LS/DYNA3D. It might be thought that it was useful to use full numerical simulation to assess the structural failure mechanisms and the informations on the energy absorption capacity, for which large or full scale experiments are difficult and not practical. The following observations from the numerical simulations can be obtained:

- Over the final simulation time t=4.5sec, ADH/PD328 model dissipated the most kinetic energy among all the models, and rate of its velocity decrease was also the steepest. The following models dissipated more kinetic energies sequently: PAUL BUCK, CONV/PD328, and ADH/PB. ADH/PD328 model can be considered to be a very crashworthy design globally.
- CONV/PD328 model is the most crashworthy design locally in that initiation of inner shell rupture occurred at the longest distance from fore bulkhead with the highest rock tip intrusion among all the models. This model had the most kinetic energy dissipation and the largest grounding resistant force at that time.
- Rupture initiation takes place as soon as the intruding rock creates a high inner shell membrane stresses. Rupture of inner shell can be delayed as long as the connectivity of whole bottom structure is much better to deform globally.
- The member of outer shell contributes to the crashworthiness more than and transverse webs in Conventional double hull bottom structures, whereas the members of longitudinal webs, than outer shell member in Advanced Double Hull ones.

- For the future study, realization of optimized double hull bottom against grounding will be performed, through the simulations using more various bottom designs, various arrangements of members, and change of their sizes and thicknesses.

References

[1] H. Lenselink et. al., "A 3-dimensional numerical simulation of the full scale Dutch-Japanese full scale ship collision tests with ALE fluid-structure interaction", FEM WORLD CONFERENCE, Monte Carlo, November 1993.

[2] J.Y. Kim et. al., "Behavior of double hull VLCCs in collision", PRADS '95, September 1995.

[3] Ou Kitamura, "Comparative study on collision resistance of side structure", Int. Conference on Designs and Methodologies for Collision and Grounding Protection of Ships, August 1996.

[4] S.G. Lee, Y.K. Chung, "A study on the critical collision speed of double hull VLCC", Proc. of the 7th Int. Offshore and Polar Eng. Conference, Honolulu, Hawaii, May 1997.

[5] J.S. Che et. al., "Numerical simulations of double hull VLCC in grounding events", Samsung Heavy Industry, December 1994.

[6] James L. Rodd and Jerome P. Sikora, "Double hull grounding experiments", Proc. of the 5th Int. Offshore and Polar Eng. Conference, The Hague, The Netherlands, June 1995.

[7] James L. Rodd, "Large scale tanker grounding experiments", Proc. of the 6th Int. Offshore and Polar Eng. Conference, Los Angeles, USA, May 1996.

[8] James L. Rodd, "Observations on Conventional and Advanced Double Hull grounding experiments", SNAME/SNAJ Conference, August 1996.

[9] G.R. Cowper and P.S. Symonds, "Strain-hardening and strain-rate effects in the impact loading of cantilever beams", Tech. Report No. 28, Brown University, Rhode Island, 1957.